

Efficient quantum memory and entanglement between light and an atomic ensemble using magnetic fields

Christine A. Muschik¹, Klemens Hammerer¹, Eugene S. Polzik^{2,3}, J. Ignacio Cirac¹

¹Max-Planck-Institut für Quantenoptik, Hans-Kopfermann-Strasse, D-85748 Garching, Germany

²QUANTOP, Danish Research Foundation Center for Quantum Optics, DK 2100 Copenhagen, Denmark

³Niels Bohr Institute, DK 2100 Copenhagen, Denmark

We present two protocols, one for the storage of light in an atomic ensemble and the subsequent retrieval, and another one for the generation of entanglement between light and atoms. They rely on two passes of a single pulse through the ensemble, Larmor precessing in an external field. Both protocols work deterministically and the relevant figures of merit - such as the fidelity or the EPR variance - scale exponentially in the coupling strength. We solve the corresponding Maxwell-Bloch equations describing the scattering process and determine the resulting input-output relations which only involve one relevant light mode that, in turn, can be easily accessed experimentally.

PACS numbers: 03.67.Mn, 32.80.Qk

I. INTRODUCTION

Recent years have seen significant progress towards an efficient quantum interface between light pulses carrying quantum information and atomic ensembles suitable for storing and processing this information. Two approaches based on probabilistic photon detection [1, 2, 3] or on deterministic homodyne measurements [4, 5] have been developed. Of particular importance in the context of quantum information are means to swap the state of light and atoms - enabling a quantum memory for light - and to create Einstein-Podolsky-Rosen (EPR) type of entanglement of light and atoms - the basic resource for quantum teleportation.

Concerning the quest for a quantum memory, an important experimental advance was the recent demonstration of the storage of weak coherent light pulses in atoms [4], based on a Quantum Non Demolition (QND) interaction, measurement of light and feedback on atoms. However, reliable retrieval of the stored state by means of the same protocol would require the use of short pulses of squeezed light which are difficult to couple to atomic ensembles in an efficient way. The design of less demanding protocols for storage and retrieval of states of light remained a challenge, also from a theoretical perspective. Several protocols have been put forward, all relying on multiple passes of light through the atomic ensemble [6, 7, 8, 9, 10, 11]. The most efficient of these schemes, complying with the experimental requirement to use Larmor precessing atomic spins, require eight passes of a single pulse [10] or two pulses each crossing twice an atomic cell [11]. In this paper we present a protocol, which consists of only *two* passes of a *single* pulse and achieves a state exchange of light and atoms scaling *exponentially* in the coupling strength κ , defined operationally as the signal to noise ratio of the underlying QND interaction. This scheme allows one to perform the complete transfer of a quantum state of light onto atoms and back under modest experimental conditions, as we show for both, coherent states as well as arbitrary superpositions of vac-

uum and a single photon Fock state.

Moreover, the same double pass setup serves with a slightly changed geometry as a deterministic source of EPR entanglement between light and atoms. The entanglement scales thereby again exponentially in κ . Together, these two protocols add to the growing toolbox for quantum information processing with room temperature atomic vapors, which has already provided the possibility to entangle two atomic ensembles via a Bell-measurement on two Larmor precessing spins [12]. In combination these tools undoubtedly pave the way towards numerous relevant applications, of which the demonstration of a complete quantum memory and quantum teleportation are just the most immediate.

To be more specific, the setup of both protocols consists of an ensemble placed in an external magnetic field with large spin polarization along the axis of this field, such that the transverse spin components precess at frequency Ω . A coherent pulse is directed through the atomic sample such, that it crosses it twice under an angle of 90 degrees in the plane orthogonal to the axis of the magnetic field. The length d of the loop in the optical path is small, such that Larmor precession is frozen on a time scale $d/c \ll \Omega^{-1}$, but the pulse length is large as compared to the Larmor period, $T \gg \Omega^{-1}$. Under these conditions and the assumption that $\Omega T \gg \kappa^2$, which is well fulfilled in current experiments, we carefully solve the Maxwell-Bloch equations describing the dynamics of this scattering process. We identify the relevant light modes, which can be stored and retrieved or get entangled with atoms and characterize their temporal profile. The central frequency of these modes lies at the upper or lower sideband of the carrier frequency, which is to be expected given the splitting of ground state levels of Ω , and their slowly varying amplitude is exponential of the form $\exp(\pm \kappa^2 t/2T)$. The modes can thus be easily accessed. Note that this setup is, apart from the magnetic field, similar to the one treated in [10]. It is precisely the presence of the magnetic field what enables us to achieve our results with the simple setup described above.

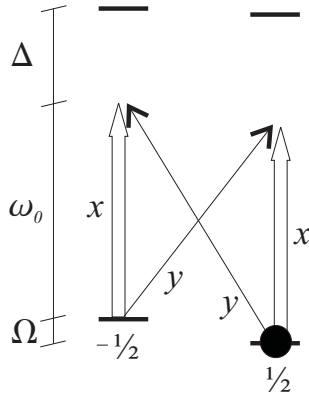


FIG. 1: Relevant internal levels with quantization along \hat{x} . Thick arrows represent the strong coherent field in \hat{x} polarization, thin arrows indicate the quantum field in \hat{y} polarization.

The rest of the paper is organized as follows. In section II we introduce the basic idea of our protocol and summarize the central results. In section III and IV we provide the detailed derivation for the quantum memory and the EPR source respectively. These sections are supplemented by two appendices. Finally, section V deals with sources of noise under realistic conditions.

II. BASIC IDEA AND CENTRAL RESULTS

We consider an atomic ensemble in a magnetic field interacting with a pulse of light propagating along \hat{z} . The atomic sample is assumed to be spin polarized along \hat{x} , while the magnetic field is orientated along the opposite direction. The pulse of light consists of a strong coherent \hat{x} -polarized component of central frequency ω_0 , which is detuned by Δ from the atomic transition, and a copropagating quantum field in \hat{y} polarization. Atoms have a relevant internal structure as shown in figure 1. With \hat{x} being the quantization axis, the classical light field drives the $m = \pm 1/2 \rightarrow m' = \pm 1/2$ transitions, while the copropagating quantum field couples to the $m = \mp 1/2 \rightarrow m' = \pm 1/2$. In the case of a dominant ground state population of $m = 1/2$ levels, creation and annihilation operators of collective atomic excitations can be defined by $b^\dagger = \sum_i | -1/2 \rangle \langle 1/2 | / \sqrt{N_A}$ and b , respectively, where N_A is the total number of atoms in the ensemble. Creation of an atomic excitation will then be accompanied by the absorption (emission) of a photon at frequency $\omega_0 + \Omega$, ($\omega_0 - \Omega$), that is, at the upper (lower) sideband, where Ω is the Larmor frequency. Note that only the polarization, and not the energy of the sideband photons are relevant, so the notion of upper/lower sideband is rather arbitrary. Although we will finally deal with light interacting with atoms in free space, it is instructive to consider first the case, where atoms are placed inside a cavity sup-

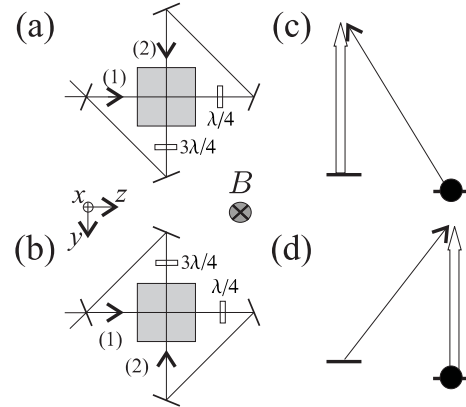


FIG. 2: Setups for having (a) a beam splitter or (b) a two mode squeezing like dynamics. (c) and (d) show the effective transitions.

porting both sideband modes. Related setups employing cavities are considered in [13, 14]. We assume in the following that the cavity life time is much smaller than the Larmor period Ω^{-1} and let the creation operators for the upper and lower sideband be given by a_{us}^\dagger and a_{ls}^\dagger respectively. In the dispersive limit, the effective Hamiltonian describing the interaction is given by $H \propto (b a_{us}^\dagger - b^\dagger a_{ls}^\dagger + \text{h.c.})$, where the signs follow from Clebsch-Gordan coefficients. Note that if ground state levels were degenerate, such that $a_{us} = a_{ls} \equiv a$, the Hamiltonian would be $H \propto (b - b^\dagger)(a - a^\dagger)$, which is well known from the theory of quantum non-demolition (QND) measurements of atomic spins. Including Zeeman splitting, the interaction consists of a passive and an active part, $H = H_{\text{pas}} - H_{\text{act}}$, where the passive part is a beam splitter Hamiltonian $H_{\text{pas}} \propto b a_{us}^\dagger + \text{h.c.}$ and acts only on the upper sideband, while the active part $H_{\text{act}} \propto b^\dagger a_{ls}^\dagger + \text{h.c.}$ can be identified with a two-mode-squeezing interaction, which involves exclusively the lower sideband. Now, either of these two interactions can be selected in one of the setups shown in figure 2a or 2b. The interaction in every second pass will again be given by H but with phase changes $a_{ls(us)} \rightarrow i a_{ls(us)}$, due to the $\lambda/4$ wave plate, and $b \rightarrow \pm i b$, due to the change of the direction of light propagation, where the upper sign holds for setup in figure 2a and the lower for 2b. The resulting Hamiltonian is $H'_\pm \propto \pm (b a_{us}^\dagger + b^\dagger a_{ls}^\dagger + \text{h.c.})$. Together, we get for setup 2a an interaction $H + H'_+ = H_{\text{pas}}$ and for 2b $H + H'_- = -H_{\text{act}}$. In either setup one of the two Λ -type transitions in figure 1 is canceled by interference, and one is left with the transitions shown in figures 2c and 2d. Note that these configurations remind of the Raman scattering processes put forward in [15] for the realization of a quantum repeater. Without a cavity, in setups as shown in figure 3, the effects still persists, as we will show by solving the corresponding Maxwell-Bloch equations. In contrast to the dynamics inside a cavity,

where Larmor precession of the atomic spin is not crucial, it is well so for propagation in free space. This can be understood by noting that both setups shown in figure 3, possess a certain asymmetry in how the two transverse spin components in \hat{y} and \hat{z} direction are affected by light. This was calculated in great detail in [10], where amongst others the setup of figure 3 was examined without magnetic field. We emphasize that Larmor precession helps to remove this asymmetry.

In the rest of this section we collect the results for both, the quantum memory and the two mode squeezing protocol. This will be done in the language of canonical operators $x_A = (b + b^\dagger)/\sqrt{2}$ and $p_A = -i(b - b^\dagger)/\sqrt{2}$ and likewise for light, since solutions to Maxwell Bloch equations are more conveniently derived in this formalism.

Quantum memory Within the memory scheme, figure 3a, the transfer of a quantum state of light onto atoms or vice versa approaches perfect mapping exponentially in the coupling strength. We have

$$\begin{pmatrix} x_A^{out} \\ p_A^{out} \end{pmatrix} = e^{-\frac{\kappa^2}{2}} \begin{pmatrix} x_A^{in} \\ p_A^{in} \end{pmatrix} + \sqrt{1 - e^{-\kappa^2}} \begin{pmatrix} x_{L+}^{in} \\ p_{L+}^{in} \end{pmatrix},$$

for the write-in procedure, where $x_A^{in/out}$ and $p_A^{in/out}$ are the atomic input/output quadratures of the scheme and $x_{L+}^{in/out}$ and $p_{L+}^{in/out}$ refer to the write-in light mode. It lies at the upper sideband (according to the configuration considered above) and is modulated by a slowly varying envelope with an exponential profile, which is a propagation effect. For the retrieval the inverse accented light mode $x_{L-}^{in/out}$ and $p_{L-}^{in/out}$ is used and we have

$$\begin{pmatrix} x_{L-}^{out} \\ p_{L-}^{out} \end{pmatrix} = -\sqrt{1 - e^{-\kappa^2}} \begin{pmatrix} x_A^{in} \\ p_A^{in} \end{pmatrix} + e^{-\frac{\kappa^2}{2}} \begin{pmatrix} x_{L+}^{in} \\ p_{L+}^{in} \end{pmatrix}.$$

Note that for large κ the state exchange is perfect. It is remarkable that both pairs of input-output relations have a form which reminds of a decoherence process, with the important difference that we have modes in place of Langevin noise operators, which can be controlled at will. The Fidelity for the complete state transfer - write in and subsequent retrieval of a state of light- is given in figure 4(a) and (b) for coherent input states and light qubits respectively.

EPR source The active version of the protocol, figure 3b, generates correlations between atoms and light, which grow exponentially in the coupling. One can define interspecies EPR modes

$$\begin{aligned} x_1 &= \frac{1}{\sqrt{2}}(x_A - p_{L+}), & p_1 &= \frac{1}{\sqrt{2}}(p_A + x_{L+}), \\ x_2 &= \frac{1}{\sqrt{2}}(x_A + p_{L+}), & p_2 &= \frac{1}{\sqrt{2}}(p_A - x_{L+}). \end{aligned}$$

where \tilde{x}_{L+} , \tilde{p}_{L+} and \tilde{p}_{L-} , \tilde{p}_{L-}^{in} refer to light modes which resemble the modes introduced above apart from the fact that they involve the lower sideband. x_1 and p_2 are

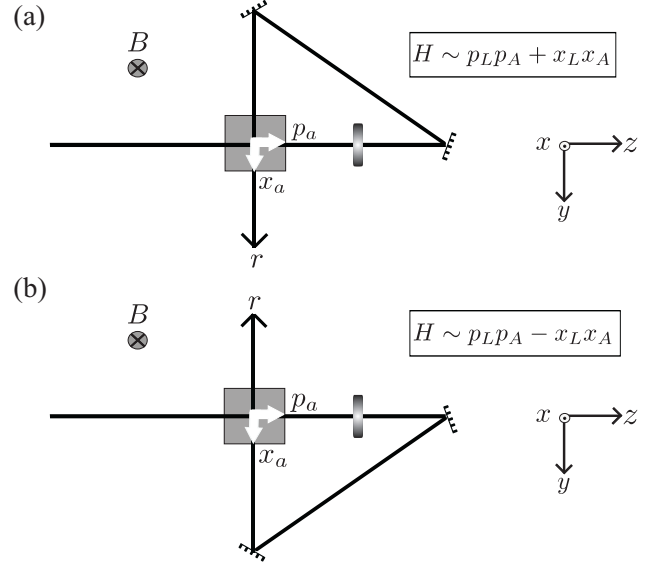


FIG. 3: Schemes for realization of a quantum memory (a) and a source of EPR entanglement (b). (a) In the first pass a $p_L p_A$ -interaction occurs. Subsequently the pulse is sent through a $\frac{1}{4}$ - plate, which interchanges x_L and p_L . The pulse is reflected back onto the sample. This happens at a timescale much shorter than the Larmor precession of the atoms. Therefore the transverse components of the collective spin can be assumed to remain in their place to a very good approximation. Finally the pulse passes the atoms along \hat{y} . Due to the changed geometry the atomic quadratures are also interchanged. $p_A \rightarrow x_A$ and $x_A \rightarrow -p_A$, which means, that the light field couples to x_A in it's second passage, hence leading to a $x_L x_A$ -interaction. In (b) the changed geometry introduces a different sign in the exchange of atomic quadratures, which leads to a $-x_L x_A$ interaction in the second pass.

squeezed, while x_2 and p_1 are antisqueezed,

$$\begin{aligned} (\Delta x_1)^2 &= (\Delta p_2)^2 = e^{-2z}, \\ (\Delta p_1)^2 &= (\Delta x_2)^2 = e^{2z}, \end{aligned}$$

where $z = \cosh^{-1}(e^{\frac{\kappa^2}{2}})$. The EPR variance of the generated state is depicted in figure 5.

The results presented above will be derived in the following sections. We remark that each protocol can be realized involving either the upper or the lower sideband. The sideband mode involved can be changed by either inverting the ground state polarization or changing the orientation of the magnetic field. Losses will be considered in section V and it will be shown that the proposed protocols are robust against the dominant sources of noise.

III. QUANTUM MEMORY

The following calculation will be done by means of canonical operators. For atoms canonical variables are

defined by means of the Holstein-Primakoff transformation and approximation [16]. Via the Holstein-Primakoff transformation spin-eigenstates are mapped onto harmonic oscillator-eigenstates. The Holstein-Primakoff approximation allows one to treat the initial coherent atomic spin state as harmonic oscillator ground state and to define the canonical atomic variables x_A and p_A corresponding to the \hat{y} and \hat{z} component of the collective angular momentum J , $x_A = J_y/\sqrt{\langle J_x \rangle}$ and $p_A = J_z/\sqrt{\langle J_x \rangle}$. The light field in \hat{y} -polarization is described by spatially localized modes

$$\begin{aligned} x_L(r) &= \frac{1}{\sqrt{4\pi}} \int_b d\omega (a_\omega e^{-i(\omega_0 - \omega)r/c} + h.c.), \\ p_L(r) &= -\frac{i}{\sqrt{4\pi}} \int_b d\omega (a_\omega e^{-i(\omega_0 - \omega)r/c} - h.c.), \end{aligned} \quad (1)$$

where the range of integration b is a small bandwidth around the carrier frequency ω_0 containing Ω . The spatial argument r refers to the distance along the optical path shown in figure 3 and we have $[x_L(r), p_L(r')] = i\hbar\delta(r - r')$, where c is the speed of light. Within this description the Hamiltonian for the off-resonant scattering interaction takes the form $H \propto p_L p_A$ [17]. Detailed descriptions can be found in [18] and [19].

A. Write-in

The double-pass interaction in setup 3a can be described by

$$H = H_{atoms} + H_{light} + V_1 + V_2.$$

$H_{atoms} = \frac{\hbar\Omega}{2}(x_A^2 + p_A^2)$ refers to Zeeman-splitting of the atomic ground state causing Larmor precession of the transverse spin components represented by x_A and p_A . The interaction terms V_1 and V_2 account for the off-resonant scattering interaction in the first and second passage of the pulse respectively. They are given by

$$V_1 = \frac{\hbar\kappa}{\sqrt{T}} p_A p_L(0) \quad \text{and} \quad V_2 = \frac{\hbar\kappa}{\sqrt{T}} x_A x_L(d),$$

where T is the duration of the pulse. V_1 was already introduced. V_2 describes basically the same kind of interaction, but due to the changed geometry in the second pass atomic quadratures are interchanged $p_A \rightarrow x_A$. Since the beam is sent through a quarter wave plate between it's passes through the atomic sample, light quadratures are interchanged as well $p_L \rightarrow x_L$. The arguments of the light-operators in V_1 and V_2 indicate that the first scattering interaction occurs at $r = 0$, while the second interaction happens after the light has travelled some distance d in the small loop between the mirrors. The length of the laser pulse is hereby supposed to be large compared with the distance within the loop. In typical experiments pulses of a length of several hundred km are used, therefore the pulse encounters itself in the sample. H_{light} represents free propagation of light. It acts on light quadratures like $\partial_t x_L(r) = \frac{i}{\hbar} [H_{light}, x_L(r)] \cong -c\partial_r x_L(r)$, which

is a suitable approximation for the light modes defined in (1). Evaluating the Heisenberg equations gives

$$\begin{aligned} \partial_t x_A(t) &= \Omega p_A(t) + \frac{\kappa}{\sqrt{T}} p_L(0, t), \\ \partial_t p_A(t) &= -\Omega x_A(t) - \frac{\kappa}{\sqrt{T}} x_L(d, t), \\ (\partial_t + c\partial_r) x_L(r, t) &= \frac{\kappa c}{\sqrt{T}} p_A(t)\delta(r), \\ (\partial_t + c\partial_r) p_L(r, t) &= -\frac{\kappa c}{\sqrt{T}} x_A(t)\delta(r - d). \end{aligned}$$

By performing the variable transformation $\xi = ct - r$ we obtain the Maxwell-Bloch equations

$$\partial_t x_A(t) = \Omega p_A(t) + \frac{\kappa}{\sqrt{T}} \bar{p}_L(ct, t), \quad (2)$$

$$\partial_t p_A(t) = -\Omega x_A(t) - \frac{\kappa}{\sqrt{T}} \bar{x}_L(ct - d, t), \quad (3)$$

$$\partial_t \bar{x}_L(\xi, t) = \frac{\kappa c}{\sqrt{T}} p_A(t)\delta(ct - \xi), \quad (4)$$

$$\partial_t \bar{p}_L(\xi, t) = -\frac{\kappa c}{\sqrt{T}} x_A(t)\delta(ct - \xi - d). \quad (5)$$

Light modes in new variables are denoted by a bar $\bar{x}_L(\xi, t) = x_L(ct - \xi, t)$. The light variable argument ξ refers to a coordinate system which is fixed on the light pulse. It allows to denote easily particular pieces on the pulse. At a certain instant of time ξ labels the pieces according to their position starting with the piece, which enters the atomic sample first.

This set of coupled differential equations has now to be solved. As a first step we treat the equations for light. In the first pass a $p_L p_A$ -interaction occurs and x_L picks up some p_A contribution. The delta function in (4) reflects the fact that a certain piece ξ of the pulse gets a contribution from the atomic state at $t = \xi/c$ (which is the instant of time the piece in consideration passes by). In the second pass a $x_L x_A$ -interaction occurs, and the atomic x -quadrature is written onto p_L . A piece ξ of the pulse, which interacted with p_L at time ξ/c gets a contribution from x_L after it has travelled a distance d in the loop. Therefore the atomic x quadrature is picked up at $t = \xi/c + d/c$ which is indicated by the delta-function in equation (5). By integrating equations (4) and (5) formally these delta functions turn into Heaviside functions,

$$\begin{aligned} \bar{x}_L(\xi, t) &= \bar{x}_L(\xi, 0) + \frac{\kappa c}{\sqrt{T}} \int_0^t d\tau p_A(\tau)\delta(c\tau - \xi) \\ &= \bar{x}_L(\xi, 0) + \frac{\kappa}{\sqrt{T}} p_A(\xi/c)\Theta(t - \xi/c), \\ \bar{p}_L(\xi, t) &= \bar{p}_L(\xi, 0) - \frac{\kappa c}{\sqrt{T}} \int_0^t d\tau x_A(\tau)\delta(c\tau - \xi - d) \\ &= \bar{p}_L(\xi, 0) - \frac{\kappa}{\sqrt{T}} x_A(\xi/c + d/c)\Theta(t - \xi/c - d/c). \end{aligned}$$

Now $\bar{p}_L(ct, t)$ and $\bar{x}_L(ct - d, t)$ are calculated, since these expressions have to be plugged into the atomic differential equations (2) and (3). The fact that the arguments

are different for x_L and p_L can be understood by considering the processes going on in the course of the double pass scheme. During the $p_L p_A$ -interaction in the first passage x_A picks up some p_L contribution. If we consider this process at a certain instant of time t , the relevant piece of the pulse is the one, which is at $r = 0$, which means for which $\xi = ct - r = ct$. p_A is acted upon by x_L in the second pass by the piece of the pulse which passes $r = d$ at time t . So it gets a contribution from $\bar{p}_L(ct - d, t)$. One finds

$$\begin{aligned}\bar{x}_L(ct - d, t) &= \bar{x}_L(ct - d, 0) + \frac{\kappa}{\sqrt{T}} p_A(t - d/c) \Theta(d/c) \\ &= \bar{x}_L(ct - d, 0) + \frac{\kappa}{\sqrt{T}} p_A(t - d/c), \\ \bar{p}_L(ct, t) &= \bar{p}_L(ct, 0) - \frac{\kappa}{\sqrt{T}} x_A(t + d/c) \Theta(-d/c) \\ &= \bar{p}_L(ct, 0).\end{aligned}$$

Note that $\bar{p}_L(ct, t)$ is conserved. This feature is due to the time-delay in the loop and will turn out to be crucial for the characteristic exponential behavior of the whole scheme. After inserting these results into (2) and (3) the atomic differential equations read

$$\begin{aligned}\partial_t x_A(t) &= \Omega p_A(t) + \frac{\kappa}{\sqrt{T}} \bar{p}_L(ct, 0), \\ \partial_t p_A(t) &= -\Omega x_A(t) - \frac{\kappa}{\sqrt{T}} \bar{x}_L(ct - d, 0) - \frac{\kappa^2}{T} p_A(t - d/c).\end{aligned}$$

Now we assume $d/c \ll \Omega^{-1}$, such that the elapsed time during the run in the loop is definitely much shorter than any other relevant process. d/c can be assumed to be of the order of ns while atoms rotate slowly with a Larmor period of the order of μs . With this approximation

$$\begin{aligned}\partial_t \begin{pmatrix} x_A(t) \\ p_A(t) \end{pmatrix} &= \left\{ \Omega \begin{pmatrix} 0 & 1 \\ -1 & 0 \end{pmatrix} - \frac{\kappa^2}{T} \begin{pmatrix} 0 & 0 \\ 0 & 1 \end{pmatrix} \right\} \begin{pmatrix} x_A(t) \\ p_A(t) \end{pmatrix} \\ &\quad + \frac{\kappa}{\sqrt{T}} \begin{pmatrix} \bar{p}_L(ct, 0) \\ -\bar{x}_L(ct, 0) \end{pmatrix}. \quad (6)\end{aligned}$$

This differential equation consists of a homogeneous part and a driving term. The first term of the homogeneous part - being proportional to the Larmor frequency - reflects the fact that atoms turn with Ω in the external magnet field. The second term in the homogeneous part represents damping of p_A . Although only one quadrature is damped, the effect is distributed among both quadratures by Larmor precession. This leads to a symmetry between x and p , which is a characteristic feature of our proposal. The solution to the differential equation is

$$\begin{aligned}\begin{pmatrix} x_A(t) \\ p_A(t) \end{pmatrix} &= A(t) \begin{pmatrix} x_A(0) \\ p_A(0) \end{pmatrix} \\ &\quad + A(t) \frac{\kappa}{\sqrt{T}} \int_0^t d\tau A^{-1}(\tau) \begin{pmatrix} \bar{p}_L(ct, 0) \\ -\bar{x}_L(ct, 0) \end{pmatrix},\end{aligned}$$

where $A(t) = e^{Gt}$, $G = \Omega \begin{pmatrix} 0 & 1 \\ -1 & 0 \end{pmatrix} - \frac{\kappa^2}{T} \begin{pmatrix} 0 & 0 \\ 0 & 1 \end{pmatrix}$

is the homogeneous solution. We suppose $\Omega T \gg \kappa^2$, which matches experimental conditions, since typically $\Omega T \approx 300$ while κ^2 is of order unity. With this assumption

$$A(t) = e^{-\frac{\kappa^2 t}{2T}} R^{-1}(t),$$

where $R^{-1}(t)$ is an orthogonal matrix,

$$R^{-1}(t) = \begin{pmatrix} \cos(\Omega t) & \sin(\Omega t) \\ -\sin(\Omega t) & \cos(\Omega t) \end{pmatrix}.$$

The inverse is taken for later convenience. Therefore the atomic time evolution is given by

$$\begin{pmatrix} x_A(t) \\ p_A(t) \end{pmatrix} = e^{-\frac{\kappa^2 t}{2T}} R^{-1}(t) \begin{pmatrix} x_A^{in} \\ p_A^{in} \end{pmatrix} + e^{-\frac{\kappa^2 t}{2T}} R^{-1}(t) \frac{\kappa}{\sqrt{T}} \int_0^t d\tau e^{\frac{\kappa^2 \tau}{2T}} R(\tau) \begin{pmatrix} \bar{p}_L(ct, 0) \\ -\bar{x}_L(ct, 0) \end{pmatrix}. \quad (7)$$

Now the atomic output quadratures $x_A^{out} = x_A(T)$ and $p_A^{out} = p_A(T)$ can be directly written down. With the assumption $\Omega T = 2\pi n$ for some natural number n ,

$$\begin{pmatrix} x_A^{out} \\ p_A^{out} \end{pmatrix} = e^{-\frac{\kappa^2}{2}} \begin{pmatrix} x_A^{in} \\ p_A^{in} \end{pmatrix} + e^{-\frac{\kappa^2}{2}} \frac{\kappa}{\sqrt{T}} \int_0^T dt e^{\frac{\kappa^2 t}{2T}} R(t) \begin{pmatrix} \bar{p}_L(ct, 0) \\ -\bar{x}_L(ct, 0) \end{pmatrix}.$$

The atomic output-quadratures consist of some atomic input contribution which is damped exponentially with κ^2 and an additional light contribution which they pick up during the scattering interaction. The definition of the appropriate light-mode can be taken from this result right away,

$$\begin{pmatrix} x_{L+}^{in} \\ p_{L+}^{in} \end{pmatrix} = \frac{\kappa}{\sqrt{T} \sqrt{e^{\kappa^2} - 1}} \int_0^T dt e^{\frac{\kappa^2 t}{2T}} R(t) \begin{pmatrix} \bar{p}_L(ct, 0) \\ -\bar{x}_L(ct, 0) \end{pmatrix}, \quad (8)$$

where the prefactor assures normalization such that $[x_{L+}^{in}, p_{L+}^{in}] = i$. This new defined light mode is essentially the upper sideband mode x_{us} , p_{us} , which is given by

$$\begin{pmatrix} x_{us}^{in} \\ p_{us}^{in} \end{pmatrix} = \frac{1}{\sqrt{T}} \int_0^T dt R(t) \begin{pmatrix} \bar{p}_L(ct, 0) \\ -\bar{x}_L(ct, 0) \end{pmatrix}. \quad (9)$$

The only difference is given by the fact that the stored mode x_{L+}^{in}, p_{L+}^{in} is defined with a slowly varying envelope of the form $\exp(+\kappa^2 t/2T)$. The index "+" refers to the sign of the argument in this exponential function (later on we will also have to deal with corresponding "-" modes). With use of (8) the atomic input-output relations can be written in a compact form

$$\begin{pmatrix} x_A^{out} \\ p_A^{out} \end{pmatrix} = e^{-\frac{\kappa^2}{2}} \begin{pmatrix} x_A^{in} \\ p_A^{in} \end{pmatrix} + \sqrt{1 - e^{-\kappa^2}} \begin{pmatrix} x_{L+}^{in} \\ p_{L+}^{in} \end{pmatrix}. \quad (10)$$

These equations describe the write-in process for a signal, which is encoded at the mode described above. Remarkably, mapping of such a quantum state of light onto atoms approaches perfect read-in exponentially in the coupling strength. This arises from the fact, that in the course of the double pass scattering interaction x_L picks up some contribution from the atomic p -quadrature, while p_L in contrast is conserved. Therefore we do not get a rotating term in the basic differential equation (6), which would lead to sines and cosines in the solution, as we would expect for a beam splitter like interaction, but an exponential effect, which is characteristic for the setup.

B. Read-out

In order to perform the read-out, a pulse of light has to be sent through the double-pass setup, just like for the write-in procedure, but since we are now looking at the reverse process, the appropriate light mode for this task has to be accented in an inverse fashion. While in the write-in process the rear part of the pulse was emphasized, now the front part of the pulse has to be weighted in order to pick up atomic information best. As the exponent in the mode definition is negative this read-out mode will be denoted by a minus sign. Since we now deal with a new beam of light which is independent from the write-in pulse, read-out beam variables carry an accent,

$$\begin{pmatrix} \dot{x}_{L-}^{in} \\ \dot{p}_{L-}^{in} \end{pmatrix} = \frac{\kappa}{\sqrt{T}\sqrt{1-e^{-\kappa^2}}} \int_0^T dt e^{-\frac{\kappa^2 t}{2T}} R(t) \begin{pmatrix} \dot{p}_L(ct, 0) \\ -\dot{x}_L(ct, 0) \end{pmatrix},$$

with a new normalization constant $\kappa/(\sqrt{T}\sqrt{1-e^{-\kappa^2}})$. The input-output relations for this mode can be derived by changing the time argument of light operators from 0 to T , reflecting the fact that we now look at the light quadratures after the whole pulse run through the atomic sample

$$\begin{pmatrix} \dot{x}_{L-}^{out} \\ \dot{p}_{L-}^{out} \end{pmatrix} = \frac{\kappa}{\sqrt{T}\sqrt{1-e^{-\kappa^2}}} \int_0^T dt e^{-\frac{\kappa^2 t}{2T}} R(t) \begin{pmatrix} \dot{p}_L(ct, T) \\ -\dot{x}_L(ct, T) \end{pmatrix}.$$

To evaluate this expression in terms of input-operators the integrated versions of equations (4) and (5)

$$\begin{aligned} \dot{x}_L(\xi, t) &= \dot{x}_L(\xi, 0) + \frac{\kappa}{\sqrt{T}} p_A(\xi/c) \Theta(t - \xi/c), \\ \dot{p}_L(\xi, t) &= \dot{p}_L(\xi, 0) - \frac{\kappa}{\sqrt{T}} x_A(\xi/c) \Theta(t - \xi/c). \end{aligned}$$

are used. Therefore

$$\begin{aligned} \begin{pmatrix} \dot{x}_{L-}^{out} \\ \dot{p}_{L-}^{out} \end{pmatrix} &= \frac{\kappa}{\sqrt{T}\sqrt{1-e^{-\kappa^2}}} \int_0^T dt e^{-\frac{\kappa^2 t}{2T}} R(t) \\ &\quad \left[\begin{pmatrix} \dot{p}_L(ct, 0) \\ -\dot{x}_L(ct, 0) \end{pmatrix} - \frac{\kappa}{\sqrt{T}} \begin{pmatrix} x_A(t) \\ p_A(t) \end{pmatrix} \Theta(T-t) \right], \\ &= \begin{pmatrix} \dot{x}_{L-}^{in} \\ \dot{p}_{L-}^{in} \end{pmatrix} - \frac{\kappa^2}{T\sqrt{1-e^{-\kappa^2}}} \int_0^T dt e^{-\frac{\kappa^2 t}{2T}} R(t) \begin{pmatrix} x_A(t) \\ p_A(t) \end{pmatrix}. \end{aligned}$$

Now the atomic time evolution (7) has to be inserted. The resulting expression can be simplified by interchanging the order of the double-integral $\int_0^T dt \int_0^t d\tau \rightarrow \int_0^T d\tau \int_\tau^T dt$. With help of equation (8) the readout output can then be written as a sum of an atomic contribution and some contribution from the plus-mode.

$$\begin{pmatrix} \dot{x}_{L-}^{out} \\ \dot{p}_{L-}^{out} \end{pmatrix} = -\sqrt{1-e^{-\kappa^2}} \begin{pmatrix} x_A^{in} \\ p_A^{in} \end{pmatrix} + e^{-\frac{\kappa^2}{2}} \begin{pmatrix} \dot{x}_{L+}^{in} \\ \dot{p}_{L+}^{in} \end{pmatrix} \quad (11)$$

Note that this expression resembles the formula for the write-in procedure with the roles of light- and atomic modes interchanged.

C. Fidelity for the complete state transfer

The fidelity for the complete state transfer is given by the overlap of the initial input state and the final output state after storage and subsequent retrieval. By inserting the output of the write-in procedure (10) into the read-out equation (11) one obtains

$$\begin{aligned} x_{L-}^{fin} &= -(1-e^{-\kappa^2})x_{L+}^{in} - e^{-\frac{\kappa^2}{2}} \sqrt{1-e^{-\kappa^2}} x_A^{in} + e^{-\frac{\kappa^2}{2}} \dot{x}_{L-}^{in}, \\ p_{L-}^{fin} &= -(1-e^{-\kappa^2})p_{L+}^{in} - e^{-\frac{\kappa^2}{2}} \sqrt{1-e^{-\kappa^2}} p_A^{in} + e^{-\frac{\kappa^2}{2}} \dot{p}_{L-}^{in}. \end{aligned} \quad (12)$$

For infinite coupling κ^2 the original input-signal is retrieved within the final quadratures of the read-out pulse $x_{L-}^{fin} = -x_{L+}^{in}$ and $p_{L-}^{fin} = -p_{L+}^{in}$, while the noise terms (atomic and read-out beam input contributions) vanish. The quantum state to be stored is supposed to be unknown. It is assumed to be taken from a certain set of possible input-states. In the following two subsections we will consider coherent input states and light qubits respectively. We will first calculate the fidelity for a single state transfer and take the average over the complete set of possible input states in the next step in each case. The results will be compared to the corresponding classical limits, i.e. the maximum average fidelity, that can be achieved by classical means [20, 21, 22, 23, 24, 25].

1. Fidelity for coherent input states

We first consider storage of a coherent state of light. The overlap between an initial state with quadratures x_{L+}^{in}, p_{L+}^{in} and the final state with $\dot{x}_{L-}^{fin}, \dot{p}_{L-}^{fin}$ is given by

$$\begin{aligned} F_{coh} &= \frac{2}{\sqrt{[1+2(\Delta\dot{x}_{L-}^{fin})^2][1+2(\Delta\dot{p}_{L-}^{fin})^2]}} \\ &\quad - \frac{(\langle x_{L+}^{in} \rangle + \langle \dot{x}_{L-}^{fin} \rangle)^2}{1+2(\Delta\dot{x}_{L-}^{fin})^2} - \frac{(\langle p_{L+}^{in} \rangle + \langle \dot{p}_{L-}^{fin} \rangle)^2}{1+2(\Delta\dot{p}_{L-}^{fin})^2}. \end{aligned} \quad (13)$$

The expectation values and variances of the final light state follow directly from (12). Since the atoms and the

read-out plus mode are initially in a vacuum state we have $\langle x_{L-}^{fin} \rangle = -(1 - e^{-\kappa^2})\langle x_{L+}^{in} \rangle$ and $\langle p_{L-}^{fin} \rangle = -(1 - e^{-\kappa^2})\langle p_{L+}^{in} \rangle$, while the variances are given by $(\Delta x_{L-}^{fin})^2 = (\Delta p_{L-}^{fin})^2 = \frac{1}{2}$, as one expects for a passive transformation. Therefore

$$F_{coh} = e^{-\frac{1}{2}(\langle x_{L+}^{in} \rangle^2 + \langle p_{L+}^{in} \rangle^2)e^{-2\kappa^2}}.$$

Now the average fidelity is computed by averaging over the complete set of all possible coherent input states. For this purpose the amplitudes x_{L+}^{in} and p_{L+}^{in} are assumed to be taken according to a Gaussian distribution centered at zero with a certain width n .

$$\begin{aligned} \bar{F}_{coh}(n, \kappa) &= \frac{1}{2\pi n} \iint d\langle x_{L+}^{in} \rangle d\langle p_{L+}^{in} \rangle e^{-\frac{\langle x_{L+}^{in} \rangle^2 + \langle p_{L+}^{in} \rangle^2}{2n}} \\ &F_{coh}(\langle x_{L+}^{in} \rangle, \langle p_{L+}^{in} \rangle, \kappa), \\ &= \frac{1}{(2 - e^{-\kappa^2} - 2\sqrt{1 - e^{-\kappa^2}} + \frac{1}{n})n}. \end{aligned}$$

Figure 4a shows the average fidelity for different widths corresponding to mean photon numbers of the distribution. The corresponding classical limit $\bar{F}_{coh}^{cl} = \frac{2n+1}{4n+1}$ [20, 21] is marked by a cross on each curve.

2. Fidelity for light qubits

Now the fidelity for light-qubits is calculated. The light-qubit input state is represented by

$$|\Psi^{in}\rangle = (\alpha + \beta a_{L+}^{\dagger in})|vac\rangle,$$

where $a_{L+}^{\dagger in} = \frac{1}{\sqrt{2}}(x_{L+}^{in} - ip_{L+}^{in})$ is the creation operator for a photon in the write-in mode. The write-in and read-out procedure is given by a passive transformation U

$$\begin{aligned} |\Psi^{fin}\rangle = U|\Psi^{in}\rangle &= (\alpha + \beta U a_{L+}^{\dagger in})|vac\rangle \\ &= (\alpha + \beta U a_{L+}^{\dagger in} U^\dagger)|vac\rangle \\ &= (\alpha + \beta a_{L-}^{\dagger fin})|vac\rangle, \quad (14) \end{aligned}$$

where $U|vac\rangle = |vac\rangle$ was used. Here $a_{L-}^{\dagger fin} = \frac{1}{\sqrt{2}}(x_{L-}^{fin} - ip_{L-}^{fin})$ is the creation operator after mapping and subsequent retrieval. It can be directly calculated, since the complete input-output relations for the light-quadratures are known. With use of equations (12)

$$a_{L-}^{\dagger fin} = -(1 - e^{-\kappa^2})a_{L+}^{\dagger in} - e^{-\frac{\kappa^2}{2}}\sqrt{1 - e^{-\kappa^2}}a_A^{\dagger in} + e^{-\frac{\kappa^2}{2}}\dot{a}_{L-}^{\dagger in}, \quad (15)$$

where $a_{L+}^{\dagger in}$, $a_A^{\dagger in}$ and $\dot{a}_{L-}^{\dagger in}$ refer to the light state to be stored, the atoms and the read-out mode respectively. The Fidelity is given by the state overlap between $|\Psi^{fin}\rangle$ and the optimal final state $|\Psi_{opt}^{fin}\rangle = (\alpha - \beta a_{L+}^{\dagger in})|vac\rangle$. By inserting (15) into expression (14) F_{qubit} can easily be determined. One obtains

$$F_{qubit} = |\langle \Psi^{fin} | \Psi_{opt}^{fin} \rangle|^2 = |(|\alpha|^2 + \{1 - e^{-\kappa^2}\}|\beta|^2)|^2.$$

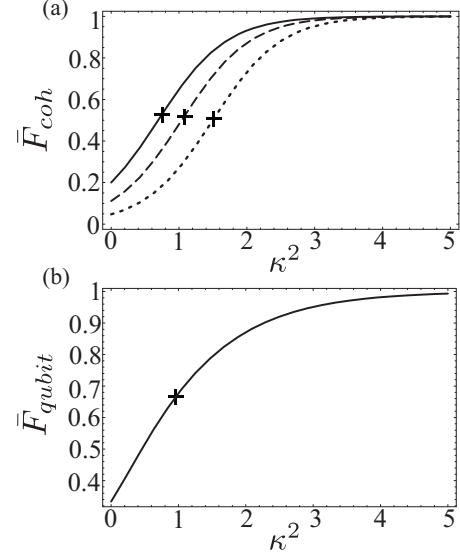


FIG. 4: Average fidelity for write-in and subsequent read-out of a light state versus coupling κ^2 . Crosses indicate the classical limit in each case. (a) Average fidelity for coherent light states according to distributions with different mean photon numbers (solid line: $n=4$, dashed line: $n=8$, dotted line: $n=20$) (b) Average fidelity for light qubits.

The average fidelity is calculated by setting $\alpha = \cos(\frac{\theta}{2})$ and $\beta = \sin(\frac{\theta}{2})e^{i\phi}$ and integrating over the whole Bloch-sphere,

$$\begin{aligned} \bar{F}_{qubit}(\kappa) &= \frac{1}{4\pi} \int_0^\pi d\theta \int_0^{2\pi} d\phi \sin(\theta) F_{qubit}(\theta, \phi) \\ &= 1 - e^{-\kappa^2} + \frac{1}{3}e^{-2\kappa^2}. \end{aligned}$$

Figure 4b shows this result. The maximal average fidelity that can be achieved for qubit states by a classical strategy $\bar{F}_{qubit}^{cl} = \frac{2}{3}$ [22, 23, 24] is indicated by a cross.

IV. TWO MODE SQUEEZING

The interaction which governs the squeezing scheme pictured in figure 3(b), is given by

$$\tilde{H} = H_{atoms} + H_{light} + V_1 - V_2.$$

This Hamiltonian differs from the one used in the memory section just by a sign in the interaction term referring to the second passage. The pulse runs along $-\hat{y}$ in the second pass of the squeezing scheme (instead of \hat{y} in the previous case) and sees therefore $-x_A$. Hence we have the minus sign in front of V_2 for the new setup.

A. Input-output relations

The atomic input-output relations can now be derived in complete analogy to section III A. By evaluating the Heisenberg equations as above we get

$$\begin{aligned} \partial_t \begin{pmatrix} x_A(t) \\ p_A(t) \end{pmatrix} &= \left\{ \Omega \begin{pmatrix} 0 & 1 \\ -1 & 0 \end{pmatrix} + \frac{\kappa^2}{T} \begin{pmatrix} 0 & 0 \\ 0 & 1 \end{pmatrix} \right\} \begin{pmatrix} x_A(t) \\ p_A(t) \end{pmatrix} \\ &+ \frac{\kappa}{\sqrt{T}} \begin{pmatrix} \bar{p}_L(ct, 0) \\ \bar{x}_L(ct, 0) \end{pmatrix}. \end{aligned}$$

With the usual approximation $\kappa^2 \ll 2\Omega T$ we obtain

$$\begin{aligned} \begin{pmatrix} x_A(t) \\ p_A(t) \end{pmatrix} &= e^{\frac{\kappa^2 t}{2T}} R^{-1}(t) \begin{pmatrix} x_A^{in} \\ p_A^{in} \end{pmatrix} \\ &+ e^{\frac{\kappa^2 t}{2T}} R^{-1}(t) \frac{\kappa}{\sqrt{T}} \int_0^t d\tau e^{-\frac{\kappa^2 \tau}{2T}} R(\tau) \begin{pmatrix} \bar{p}_L(ct, 0) \\ \bar{x}_L(ct, 0) \end{pmatrix}. \end{aligned}$$

These equations are in a significant way different from the atomic time evolution (7) in the memory scheme. Note first the signs in the arguments of the exponential functions. We now have exponential enhancement of the atomic input instead of exponential damping. Furthermore light is involved in form of a minus mode in the atomic input-output relations because of the minus sign in the exponent within the integral. Note second, that the minus sign, which was present in in front of $\bar{x}_L(ct, 0)$ in the memory scheme, does not appear in this case. Therefore the lower sideband

$$\begin{pmatrix} p_{ls}^{in} \\ x_{ls}^{in} \end{pmatrix} = \frac{1}{\sqrt{T}} \int_0^T dt R(t) \begin{pmatrix} \bar{p}_L(ct, 0) \\ \bar{x}_L(ct, 0) \end{pmatrix} \quad (16)$$

is involved instead of the upper one (9). Hence the minus mode showing up in the atomic time evolution is defined slightly differently from the memory section

$$\begin{pmatrix} \tilde{p}_{L-}^{in} \\ \tilde{x}_{L-}^{in} \end{pmatrix} = \frac{\kappa}{\sqrt{T} \sqrt{1 - e^{-\kappa^2}}} \int_0^T dt e^{-\frac{\kappa^2 t}{2T}} R(t) \begin{pmatrix} \bar{p}_L(ct, 0) \\ \bar{x}_L(ct, 0) \end{pmatrix}.$$

With use of this definition and the assumption $\Omega T = 2\pi n$ for some natural number n , the atomic input-output relations read

$$\begin{pmatrix} x_A^{out} \\ p_A^{out} \end{pmatrix} = e^{\frac{\kappa^2}{2}} \begin{pmatrix} x_A^{in} \\ p_A^{in} \end{pmatrix} + \sqrt{e^{\kappa^2} - 1} \begin{pmatrix} \tilde{p}_{L-}^{in} \\ \tilde{x}_{L-}^{in} \end{pmatrix}. \quad (17)$$

Light input-output relations for this process can be derived in analogy to the procedure in section III B. The inverse accented counter-part of the light mode used in the atomic evolution is given by

$$\begin{pmatrix} \tilde{p}_{L+}^{in} \\ \tilde{x}_{L+}^{in} \end{pmatrix} = \frac{\kappa}{\sqrt{T} \sqrt{e^{\kappa^2} - 1}} \int_0^T dt e^{\frac{\kappa^2 t}{2T}} R(t) \begin{pmatrix} \bar{p}_L(ct, 0) \\ \bar{x}_L(ct, 0) \end{pmatrix}.$$

We refer now to the same pulse as in (17), while in the derivation of the input-output relations for atoms and light in section III two independent beams were considered. We obtain

$$\begin{pmatrix} \tilde{p}_{L+}^{out} \\ \tilde{x}_{L+}^{out} \end{pmatrix} = \sqrt{e^{\kappa^2} - 1} \begin{pmatrix} x_A^{in} \\ p_A^{in} \end{pmatrix} + e^{\frac{\kappa^2}{2}} \begin{pmatrix} \tilde{p}_{L-}^{in} \\ \tilde{x}_{L-}^{in} \end{pmatrix}. \quad (18)$$

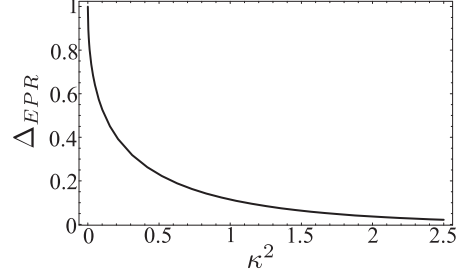


FIG. 5: Entanglement produced in the two mode squeezing scheme versus coupling κ^2 . The entanglement is hereby measured by the EPR variance Δ_{EPR} .

Please note that the input-output relations (17) and (18) are active versions of (10) and (11) respectively.

B. Creation of entanglement

As can be seen from the input-output relations for atoms and light given in equations (17) and (18) respectively, correlations between atoms and light are created which grow exponentially in the coupling strength. We define new modes appropriate to the type of correlations produced in the system by setting

$$\begin{aligned} x_1 &= \frac{1}{\sqrt{2}}(x_A - \tilde{p}_{L+}), & p_1 &= \frac{1}{\sqrt{2}}(p_A + \tilde{x}_{L+}), \\ x_2 &= \frac{1}{\sqrt{2}}(x_A + \tilde{p}_{L+}), & p_2 &= \frac{1}{\sqrt{2}}(p_A - \tilde{x}_{L+}). \end{aligned}$$

The corresponding variances can be calculated easily from (17) and (18). We get

$$\begin{aligned} (\Delta x_1)^2 &= (\Delta p_2)^2 = \left(\sqrt{e^{\kappa^2} - 1} - e^{\frac{\kappa^2}{2}} \right)^2 = e^{-2z}, \\ (\Delta p_1)^2 &= (\Delta x_2)^2 = \left(\sqrt{e^{\kappa^2} - 1} + e^{\frac{\kappa^2}{2}} \right)^2 = e^{2z}, \end{aligned}$$

with $z = \cosh^{-1}(e^{\frac{\kappa^2}{2}})$. We get a two mode squeezed state where x_1 and p_2 are squeezed, while p_1 and x_2 are antisqueezed. In the limit of infinite coupling the state becomes an EPR state in which x_A , \tilde{p}_{L+} and p_A , \tilde{x}_{L+} are perfectly correlated. For the state under consideration, the EPR-variance $\Delta_{EPR} = \frac{1}{2}(\Delta x_1^2 + \Delta p_2^2) = e^{-2z}$ is an entanglement measure [26]. For separable states $\Delta_{EPR} = 1$. For inseparable states Δ_{EPR} decreases with increasing entanglement. The amount of entanglement created in the scheme is shown in figure 5.

C. Spin squeezing

The correlations created in the proposed scheme can be used to produce atomic squeezing. This can be achieved

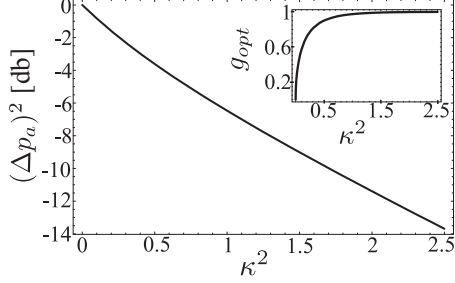


FIG. 6: Atomic squeezing $(\Delta p_a)^2$ in db versus coupling κ^2 for optimal gainfactor g_{opt} . The inset shows how the optimal gainfactor depends on the coupling.

by performing a measurement on the plus light mode and subsequent feedback onto the atomic spin based on the measurement outcome. The squeezing protocol is symmetric with respect to interchange of $\{x_A, \tilde{x}_L\}$ and $\{p_A, \tilde{x}_L\}$. Here squeezing of $(\Delta p_A)^2$ is illustrated. In order to acquire information about p_A , \tilde{x}_{L+} has to be measured. The outcome of this measurement is governed by the operator equation

$$\tilde{x}_{L+}^{out} = \sqrt{e^{\kappa^2} - 1} p_A^{in} + e^{\frac{\kappa^2}{2}} \tilde{x}_{L-}^{in}.$$

If the measurement outcome q_{L+} is obtained p_A^{out} is displaced by an amount $g q_{L+}$, where $g \in \mathbb{R}$ is some gain factor. For this feedback procedure the operator identity

$$p_A^{fb} = p_A^{out} - g \tilde{x}_{L+}^{out}$$

holds in the ensemble average, as is shown in [4, 18]. With help of the atomic input-output relations (17) and the expression for the measurement outcome above

$$p_A^{fb} = \left(e^{\frac{\kappa^2}{2}} - g \sqrt{e^{\kappa^2} - 1} \right) p_A^{in} + \left(\sqrt{e^{\kappa^2} - 1} - g e^{\frac{\kappa^2}{2}} \right) \tilde{x}_{L-}^{in}.$$

Thus the variance of this quadrature is given by

$$(\Delta p_A^{fb})^2 = \left(e^{\frac{\kappa^2}{2}} - g \sqrt{e^{\kappa^2} - 1} \right)^2 \frac{1}{2} + \left(\sqrt{e^{\kappa^2} - 1} - g e^{\frac{\kappa^2}{2}} \right)^2 \frac{1}{2}.$$

$(\Delta p_A^{fb})^2$ is now optimized with respect to the gainfactor g . We obtain

$$g_{opt} = \frac{e^{\frac{\kappa^2}{2}} \sqrt{e^{\kappa^2} - 1} + e^{\kappa^2} \sqrt{1 - e^{-\kappa^2}}}{2e^{\kappa^2} - 1},$$

$$(\Delta p_A^{fb})^2 = \frac{1}{2} \frac{1}{2e^{\kappa^2} - 1}.$$

Note that the atoms are left in a minimum uncertainty state, since

$$(\Delta x_A)^2 = \frac{1}{2} (2e^{\kappa^2} - 1) = \frac{1}{4} \frac{1}{(\Delta p_A^{fb})^2}.$$

The amount of squeezing depending on the coupling κ^2 is shown in figure 6.

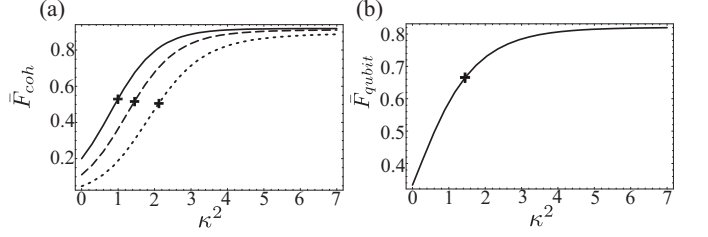


FIG. 7: Average fidelity with losses versus coupling. The atomic decay rate η and the reflection coefficient r both have a value of 7.5%. Crosses mark the corresponding classical limits. (a) Fidelity for coherent input states according to distributions with different mean photon numbers. (solid line: $n = 4$, dashed line: $n = 8$, dotted line: $n = 20$) (b) Fidelity for light qubits.

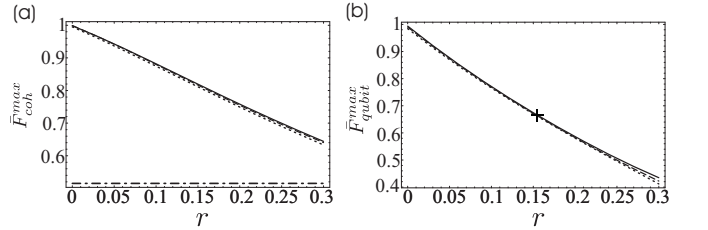


FIG. 8: Maximal attainable average fidelity for coherent input states according to a distribution with mean photon number $n = 8$ (a) and light qubits (b) versus reflection coefficient r for different atomic decay parameters η . (solid lines: $\eta = 5\%$, dashed lines: $\eta = 10\%$, dotted lines: $\eta = 25\%$) The dash-dotted line and the cross indicate the classical limits.

V. CONSIDERATION OF NOISE

We consider losses for both components of the protocol - atoms and light - and treat them perturbatively within the Gaussian formalism. Concerning the atomic sample we take transverse decoherence of the atomic spin state at a rate of $\frac{\eta}{T}$ into account. As in experiments atomic vapor is usually contained within a glass cell, the dominant source of noise concerning light are reflection losses. These affect quantum variables and classical field as well and will be characterized by the reflection coefficient r .

A. Quantum memory with noise

In this section we sum up results for write-in and read-out in the presence of losses. A detailed description of the generalized quantum memory scheme including noise is given in appendix A. Consideration of losses leads to a modification of the original write-in mode. The generalized write-in quadratures preferred by the system are

given by

$$\begin{pmatrix} x^{in} \\ p^{in} \end{pmatrix} \propto \int_0^T dt e^{\frac{wt}{2}} R(t) \left[(1-r) \begin{pmatrix} \bar{p}_L(ct,0) \\ -\bar{x}_L(ct,0) \end{pmatrix} + 2r \begin{pmatrix} \bar{p}_L(ct,0) \\ \bar{x}_L(ct,0) \end{pmatrix} \right],$$

where $w = \eta/T + \kappa^2(1-2r)/T$. Both sources of noise - reflection losses and spontaneous decay as well - give rise to a generalized exponent in the exponential modulation function. In addition to the changed envelope the light mode appearing in the atomic input-output relation is further disturbed: it lies no longer exactly at the upper sideband, but contains a small contribution from the lower one, as can be seen by comparing the expression above to (9) and (16). Since it is experimentally advantageous to encode the input signal at sideband modes, we define a generalized write-in mode (denoted by capital letters)

$$\begin{pmatrix} X_{us+}^{in} \\ P_{us+}^{in} \end{pmatrix} = \sqrt{\frac{w}{e^{wT} - 1}} \int_0^T dt e^{\frac{wt}{2}} R(t) \begin{pmatrix} \bar{p}_L(ct,0) \\ -\bar{x}_L(ct,0) \end{pmatrix},$$

which takes full account of noise concerning the exponential modulation, but lies precisely at the upper sideband. (i.e. the small orthogonal contribution from the lower one is treated as noise.) To perform the read-out, the inverse accented counter part of this mode is measured. The calculation of the fidelity is given in appendix B. Figure 7 shows the average fidelity for write-in and subsequent retrieval versus coupling for $r = \eta = 7.5\%$. Plots (a) and (b) refer to coherent input states and light qubits respectively. The corresponding classical limits are marked by crosses. As illustrated by these graphs losses decrease not only the quality of the state transfer for a given coupling strength, but limit also the attainable fidelity. The crucial limiting factor in this scheme are reflection losses. Figure 8 shows the maximum average fidelity versus r for different values of the atomic decay parameter η . Plot (a) shows results for coherent inputs, while plot (b) depicts the maximal attainable fidelity for qubits. The dash-dotted line and the cross indicate the classical limits in each case. Within moderate couplings fidelities well above the classical limit can be achieved, showing that the protocol is robust against the dominant sources of noise.

B. Two mode squeezing with noise

Consideration of noise within the two mode squeezing protocol is done along the same lines outlined in the section above. The entanglement created by the scheme in the presence of losses is depicted in figure 9(a) for $r = \eta = 0.1$. The EPR variance increases for higher values of κ^2 . An optimal value κ_{opt}^2 exists for which the proposed protocol works best and a maximal amount of entanglement is generated. Figure 9(b) shows the κ -optimized EPR variance versus r , while the dependence of κ_{opt} on the reflection coefficient is given within the inset. As can be seen from these plots atomic decay plays

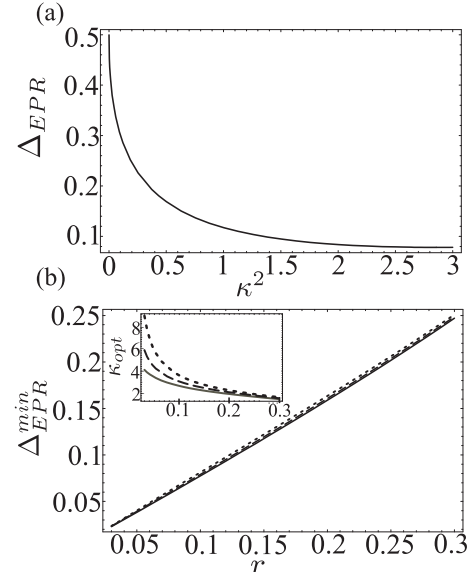


FIG. 9: (a) EPR variance Δ_{EPR} versus coupling κ^2 in the presence of losses. The reflection coefficient r and the atomic decay rate are both chosen to have a value of 10%. (b) Optimized EPR variance versus coupling for different atomic decay parameters. (solid line: $\eta = 5\%$, dashed line: $\eta = 10\%$, dotted line: $\eta = 25\%$) The inset shows how the optimal coupling κ_{opt} varies with r .

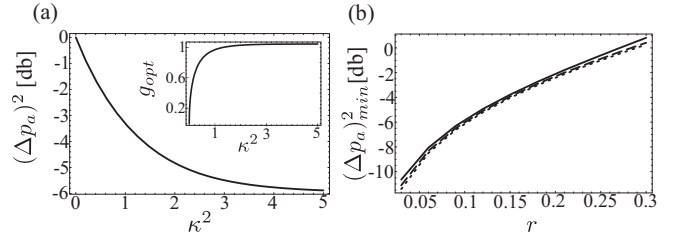


FIG. 10: (a) Spin squeezing in db versus coupling κ^2 in the presence of losses. The reflection coefficient r and the atomic decay rate both have a value of 10%. The inset shows how the optimal gain variance factor g_{opt} depends on the coupling. (b) Maximal spin squeezing versus reflection coefficient r for different atomic decay parameters. (solid line: $\eta = 5\%$, dashed line: $\eta = 10\%$, dotted line: $\eta = 25\%$).

a minor role.

Spin squeezing can be performed with a lower and limited quality in the presence of losses. In contrast to the ideal case the optimal gain factor does not approach unity with increasing coupling but converges towards a higher value which depends on the amount of losses impairing the system. Figure 10(a) shows the squeezed atomic variance in dB and the dependence of g_{opt} on the coupling for $r = \eta = 0.1$. The maximal attainable squeezing versus r is given in figure 10(b) for different atomic decay parameters.

VI. CONCLUSIONS

In conclusion we propose two protocols based on a double-pass scheme for a single atomic ensemble in a magnetic field. The first protocol provides an exponential scaling interspecies beam-splitter interaction. Therefore it is suitable for high fidelity storage and retrieval of an unknown quantum state under modest experimental conditions, as was shown for coherent input states and light qubits as well. The second protocol generates deterministically EPR entanglement between atoms and light. The proposed protocols provide therefore the ingredients to realize a variety of interesting quantum communication protocols. They are also shown to remain experimentally feasible under realistic conditions.

Acknowledgements

We thank J. Sherson, A. Sørensen and K. Mølmer for useful discussions and acknowledge funding from the EU under project FP6-511004-COVAQIAL, Integrated Project QAP and SCALA.

APPENDIX A: CONSIDERATION OF NOISE IN THE MEMORY PROTOCOL

Write-in

Atomic noise can be incorporated into the framework of section III by including decay terms in Bloch equations (2) and (3)

$$\begin{aligned} \partial_t x_A(t) &= \Omega p_A(t) + \frac{\kappa}{\sqrt{T}} \bar{p}_L(ct, t) - \frac{\eta}{2T} x_A(t) + \sqrt{\frac{\eta}{T}} f_{xA}(t), \\ \partial_t p_A(t) &= -\Omega x_A(t) - \frac{\kappa}{\sqrt{T}} \bar{x}_L(ct - d, t) \\ &\quad - \frac{\eta}{2T} p_A(t) + \sqrt{\frac{\eta}{T}} f_{pA}(t), \end{aligned} \quad (A1)$$

where f_{xA} and f_{pA} are Langevin noise operators with zero mean and $\langle f(t)f(t') \rangle = \delta(t-t')\frac{1}{2}$.

Each time light crosses one of the cell walls, reflection losses occur. This happens four times. We neglect losses due to the very first crossing, since these can be compensated by using a more intense input signal. Losses due to the second and third transit of a cell wall affect only the second scattering interaction. We take this into account by modifying the undisturbed equations for the light field quadratures to be inserted into (A1)

$$\begin{aligned} \bar{x}_L(ct - d, t) &= \bar{x}_L(ct - d, 0) + \frac{\kappa}{\sqrt{T}} p_A(t - \frac{d}{c}), \\ \bar{p}_L(ct, t) &= \bar{p}_L(ct, 0), \end{aligned}$$

by introducing light quadrature damping with a factor $2r$ (the factor 2 reflects the fact that crossing of a cell wall happens twice) and corresponding light-Langevin operators f_{xL} and f_{pL} , and obtain

$$\begin{aligned} \bar{x}_L(ct - d, t) &= \sqrt{1-2r} \left(\bar{x}_L(ct - d, 0) + \frac{\kappa}{\sqrt{T}} p_A(t - \frac{d}{c}) \right) \\ &\quad + \sqrt{2r} f_{xL}(t), \\ \bar{p}_L(ct, t) &= \bar{p}_L(ct, 0). \end{aligned}$$

$\bar{p}_L(ct, t)$ remains unchanged, since this quadrature affects the atoms only in the first passage (during the $p_L p_A$ -interaction), which means that each part of the pulse contributes before it is subjected to reflection losses. Therefore p_L is conserved as in the undisturbed case. The classical light field is impaired by reflection losses as well. Since the coupling strength of the scattering interaction is proportional to the amplitude of the classical field we have a reduced coupling $\tilde{\kappa} = \sqrt{1-2r} \kappa$ for the second ($x_L x_A$ -) interaction due to the light crossing two cell walls before it's second passage. By considering this and inserting the expressions above into equations (A1) we obtain

$$\begin{aligned} \partial_t x_A &= \Omega p_A(t) + \frac{\kappa}{\sqrt{T}} \bar{p}_L(ct, 0) - \frac{\eta}{2T} x_A(t) + \sqrt{\frac{\eta}{T}} f_{xA}(t), \\ \partial_t p_A(t) &= -\Omega x_A(t) - \frac{\tilde{\kappa}}{\sqrt{T}} \left[\sqrt{1-2r} \left(\bar{x}_L(\xi, 0) + \frac{\kappa}{\sqrt{T}} p_A(t) \right) \right. \\ &\quad \left. + \sqrt{2r} f_{xL}(t) \right] - \frac{\eta}{2T} p_A(t) + \sqrt{\frac{\eta}{T}} f_{pA}(t). \end{aligned}$$

We can ignore reflection losses arising in the very last transit through a cell wall, since the light field of the write-in beam is of no relevance after the second scattering interaction. By neglecting the time delay d/c as in section III, the atomic differential equations generalize to

$$\begin{aligned} \partial_t \begin{pmatrix} x_A(t) \\ p_A(t) \end{pmatrix} &= \left\{ \Omega \begin{pmatrix} 0 & 1 \\ -1 & 0 \end{pmatrix} - \frac{\eta}{2T} \begin{pmatrix} 1 & 0 \\ 0 & 1 \end{pmatrix} - \frac{\kappa^2(1-2r)}{T} \begin{pmatrix} 0 & 0 \\ 0 & 1 \end{pmatrix} \right\} \\ &\quad \begin{pmatrix} x_A(t) \\ p_A(t) \end{pmatrix} + \frac{\kappa}{\sqrt{T}} \begin{pmatrix} \bar{p}_L(ct, 0) \\ -(1-2r)\bar{x}_L(ct, 0) \end{pmatrix} \\ &\quad + \sqrt{\frac{\eta}{T}} \begin{pmatrix} f_{xA}(t) \\ f_{pA}(t) \end{pmatrix} + \frac{\kappa\sqrt{2r}}{\sqrt{T}} \begin{pmatrix} 0 \\ -\sqrt{1-2r}f_{xL}(t) \end{pmatrix}. \end{aligned}$$

We introduce the abbreviation $w = \eta/T + \kappa^2(1-2r)/T$, which is the generalization of the exponent κ^2/T of the previous sections and change the previous assumption $2\Omega T \gg \kappa^2$ into $2\Omega T \gg wT = \eta + \kappa^2(1-2r)$. Therefore we get the homogeneous solution $A(t) = e^{\frac{wt}{2}} R^{-1}(t)$, (where

$R(t)$ is the rotation matrix from section III) and thus

$$\begin{pmatrix} x_A^{out} \\ p_A^{out} \end{pmatrix} = e^{-\frac{wT}{2}} \begin{pmatrix} x_A^{in} \\ p_A^{in} \end{pmatrix} + e^{-\frac{wT}{2}} \frac{\kappa}{\sqrt{T}} \int_0^T dt e^{\frac{wt}{2}} R(t) \begin{pmatrix} \bar{p}_L(ct, 0) \\ -(1-2r)\bar{x}_L(ct, 0) \end{pmatrix} + e^{-\frac{wT}{2}} \sqrt{\frac{\eta}{T}} \int_0^T dt e^{\frac{wt}{2}} R(t) \begin{pmatrix} f_{xA}(t) \\ f_{pA}(t) \end{pmatrix} + e^{-\frac{wT}{2}} \frac{\kappa\sqrt{2r}}{\sqrt{T}} \int_0^T dt e^{\frac{wt}{2}} R(t) \begin{pmatrix} 0 \\ -\sqrt{1-2r}f_{xL}(t) \end{pmatrix}, \quad (\text{A2})$$

where $R(T) = \mathbb{1}$ was used. The first two lines represent atomic- and light contributions, while the third and fourth term account for atomic noise and light noise respectively. The light mode, which is naturally mapped onto the atomic sample, is no longer a modulation of the upper sideband, as can be seen from the factor $(1-2r)$ attached to $\bar{x}_L(ct, 0)$ in the second line. Since it is advantageous to encode the signal at sideband modes, the term involving the new disturbed light mode is decomposed into a generalization of the familiar plus mode connected to the upper sideband

$$\begin{pmatrix} X_{us+}^{in} \\ P_{us+}^{in} \end{pmatrix} = \sqrt{\frac{w}{e^{wT} - 1}} \int_0^T dt e^{\frac{wt}{2}} R(t) \begin{pmatrix} \bar{p}_L(ct, 0) \\ -\bar{x}_L(ct, 0) \end{pmatrix} \quad (\text{A3})$$

and a small contribution from an orthogonal plus mode lying at the lower sideband

$$\begin{pmatrix} P_{ls+}^{in} \\ X_{ls+}^{in} \end{pmatrix} = \sqrt{\frac{w}{e^{wT} - 1}} \int_0^T dt e^{\frac{wt}{2}} R(t) \begin{pmatrix} \bar{p}_L(ct, 0) \\ \bar{x}_L(ct, 0) \end{pmatrix}.$$

Generalized light modes are denoted by capital letters. With this decomposition the atomic input-output relations with noise read

$$\begin{pmatrix} x_A^{out} \\ p_A^{out} \end{pmatrix} = e^{-\frac{wT}{2}} \begin{pmatrix} x_A^{in} \\ p_A^{in} \end{pmatrix} + \sqrt{1-e^{-wT}} \frac{\kappa(1-r)}{\sqrt{wT}} \begin{pmatrix} X_{us+}^{in} \\ P_{us+}^{in} \end{pmatrix} + \sqrt{1-e^{-wT}} \frac{\kappa r}{\sqrt{wT}} \begin{pmatrix} P_{ls+}^{in} \\ X_{ls+}^{in} \end{pmatrix} + e^{-\frac{wT}{2}} \sqrt{\frac{\eta}{T}} \int_0^T dt e^{\frac{wt}{2}} R(t) \begin{pmatrix} f_{xA}(t) \\ f_{pA}(t) \end{pmatrix} + e^{-\frac{wT}{2}} \frac{\kappa\sqrt{2r}}{\sqrt{T}} \int_0^T dt e^{\frac{wt}{2}} R(t) \begin{pmatrix} 0 \\ -\sqrt{1-2r}f_{xL}(t) \end{pmatrix}. \quad (\text{A4})$$

Read-out

In order to perform the read-out, a second pulse of light is sent through the double pass scheme. Subsequently the light mode, which is the inverse accented counter-part of the mode appearing in the atomic time evolution (A2)

should be measured. Instead we choose the generalized minus mode analogous to the write-in quadratures (A3). The corresponding output quadratures are given by

$$\begin{pmatrix} \dot{X}_{us-}^{out} \\ \dot{P}_{us-}^{out} \end{pmatrix} = \sqrt{\frac{w}{1-e^{-wT}}} \int_0^T dt e^{-\frac{wt}{2}} R(t) \begin{pmatrix} \dot{\bar{p}}_L(ct, T) \\ -\dot{\bar{x}}_L(ct, T) \end{pmatrix}.$$

This can be evaluated by inserting the generalized expressions for $\dot{\bar{p}}_L(ct, T)$ and $\dot{\bar{x}}_L(ct, T)$. For $\dot{\bar{p}}_L(ct, T)$ we have

$$\dot{\bar{p}}_L(ct, T) = \sqrt{1-2r} \dot{\bar{p}}_L(ct, 0) + \sqrt{2r} \dot{f}_{pL}(t) - \frac{\tilde{\kappa}}{\sqrt{T}} x_A(t).$$

$\dot{\bar{p}}_L$ is damped after the first (p -conserving) interaction and picks up some noise in return. Subsequently it gets some x_A -contribution during the second ($x_L x_A$ -) interaction. The reduced coupling strength $\tilde{\kappa} = \sqrt{1-2r} \kappa$ accounts for the damped classical field in the second passage. $\dot{\bar{x}}_L(ct, T)$ on the other hand is given by

$$\dot{\bar{x}}_L(ct, T) = \sqrt{1-2r} \left(\dot{\bar{x}}_L(ct, 0) + \frac{\kappa}{\sqrt{T}} p_A(t) \right) + \sqrt{2r} \dot{f}_{xL}(t).$$

$\dot{\bar{x}}_L$ gets some p_A contribution during the first scattering interaction i.e. before the relevant transits through cell walls occur. Subsequently this is damped and appropriate noise is added. All together both quadratures are damped, since both carry the argument (ct, T) . This means each piece of the pulse contributes after it ran through the sample twice and has therefore already experienced the two relevant transits through cell walls. The rest of the calculation is straight forward. In the end reflection losses due to the fourth crossing of a cell wall have to be considered by damping the calculated result by a factor $\sqrt{1-r}$ and adding appropriate noise terms. The resulting input-output relations for the read-out mode are

$$\begin{pmatrix} \dot{X}_{us-}^{out} \\ \dot{P}_{us-}^{out} \end{pmatrix} = c_1 \begin{pmatrix} x_A^{in} \\ p_A^{in} \end{pmatrix} + c_2 \begin{pmatrix} \dot{X}_{us+}^{in} \\ \dot{P}_{us+}^{in} \end{pmatrix} + c_3 \begin{pmatrix} \dot{P}_{ls+}^{in} \\ \dot{X}_{ls+}^{in} \end{pmatrix} + c_4 \begin{pmatrix} \dot{X}_{us-}^{in} \\ \dot{P}_{us-}^{in} \end{pmatrix} + c_5 \begin{pmatrix} \dot{P}_{ls-}^{in} \\ \dot{X}_{ls-}^{in} \end{pmatrix} + c_6 \begin{pmatrix} F_{xA} \\ F_{pA} \end{pmatrix} + c_7 \begin{pmatrix} \check{F}_{xL} \\ \check{F}_{pL} \end{pmatrix} + c_8 \begin{pmatrix} \check{F}_{xL} \\ \check{F}_{pL} \end{pmatrix} + c_9 \int_0^T dt R(t) [e^{-wT} e^{\frac{wt}{2}} - e^{-\frac{wt}{2}}] \begin{pmatrix} 0 \\ -\dot{f}_{xL}(t) \end{pmatrix}. \quad (\text{A5})$$

The coefficients c_1 to c_9 can easily be calculated. Since we want to focus on the structure of the equation, we don't insert these prefactors in order to avoid complicated expressions. The new read-out equations differ from (11) by the appearance of noise terms (third and fourth line) and extra light modes (second line). These contributions are small and can be treated as perturbations. (F_{xA}, F_{pA}) is an atomic noise mode, while $(\check{F}_{xL}, \check{F}_{pL})$, refers to the light mode which is due to the very last reflection. It

is independent from the light mode (\hat{F}_{pL} , \hat{F}_{xL}) which accounts for the reflections happening between the scattering interactions. These intermediate reflections give also rise to terms in which only noise associated to x_L contributes. They are summarized in the expression preceded by c_8 . The appearance of light modes other than (\hat{X}_{us+} , \hat{P}_{us+}) is due to a asymmetry between the $p_L p_A$ -interaction and the $x_L x_A$ present in a realistic setup in contrast to the ideal case. The light field has to cross two glass walls between the first and the second pass (thus affecting only the $x_L x_A$ -interaction). Thus contributions from the lower sideband appear and contributions from the minus mode do not cancel as in the ideal case.

APPENDIX B: FIDELITY FOR THE COMPLETE STATE TRANSFER INCLUDING NOISE

In the following subsections the fidelity for storage and subsequent retrieval of an unknown state of light will be derived for coherent input states and light qubits respectively. Hereby reflection losses and transverse decoherence of the atomic spin state are taken into account as explained in section V.A and appendix A. The following calculations are based on the input-output relations for the complete state transfer. They are obtained by inserting equation (A4), which describes the atomic state after a noisy write-in procedure into (A5), which gives us the final retrieved light state in the presence of losses.

Fidelity for coherent input states

In order to compute the fidelity for coherent input states, means and variances of the final quadratures have to be calculated. $\langle \hat{X}_{L-}^{fin} \rangle$, $\langle \hat{P}_{L-}^{fin} \rangle$ and $(\Delta \hat{P}_{L-}^{fin})^2$, $(\Delta \hat{X}_{L-}^{fin})^2$ can be derived from the expression describing the complete state transfer by using the assumption $2\Omega T \gg wT = \eta + \kappa^2(1 - 2r)$ (which is a direct generalization from the approximation $2\Omega T \gg \kappa^2$ made in the ideal case) and help of the noise operator properties $\langle f_x \rangle = \langle f_p \rangle = \langle f_x f_p + f_p f_x \rangle = 0$ and $\langle f(t)f(t') \rangle = \delta(t - t')\frac{1}{2}$. The obtained expressions have to be inserted into equation (13), which gives the state overlap between the input-state to be stored and the final state received. By considering a gaussian distribution of width n for coherent amplitudes the average fidelity can be directly calculated as in section III C 1.

Fidelity for light qubit input states including noise

The initial qubit state $|\Psi_{in}\rangle = (\alpha + \beta a_{in}^\dagger)|vac\rangle$ is subjected to the write-in and read-out procedure which is represented by the unitary transformation U_N . We ob-

tain

$$\begin{aligned} |\Psi_{fin}\rangle &= U_N |\Psi_{in}\rangle = (\alpha + \beta U_N a_{in}^\dagger U_N^\dagger) U_N |vac\rangle \\ &= (\alpha + \beta a_{fin}^\dagger) U_N |vac\rangle. \end{aligned}$$

In contrast to the ideal case, where $U|vac\rangle = |vac\rangle$ could be used, U_N is a general Bogoliubov transformation. We remark that for $r = 0$ the state transfer can still be described by a passive transformation. The active contribution is entirely due to reflection losses. This can be understood, by noting that reflection losses occurring between the first and the second scattering interaction impair only the scattering in the second pass. Therefore the active part of the second interaction cannot compensate the active part in the first pass as in the ideal case. This leads to a term in the generalized atomic input-output relations (A4) which contains only one light quadrature and can therefore not be expressed as a mode-contribution. It plays an isolated role in the commutator relations, but adds some extra noise to the variances. Losses due to atomic decay on the other hand are included into the dynamics of the scheme in a symmetric way.

The fidelity for the complete state transfer is given by the overlap between the target state $|\Psi_{fin}^{opt}\rangle = (\alpha - \beta a_{in}^\dagger)|vac\rangle$ and the light state $|\Psi_{fin}\rangle$ which is effectively retrieved

$$F_{qubit} = |\langle \Psi_{fin}^{opt} | \Psi_{fin} \rangle|^2 = |vac(\alpha^* - \beta^* a_{in})(\alpha + \beta a_{fin}^\dagger) U_N |vac\rangle|^2. \quad (B1)$$

a_{fin}^\dagger is known, since the input-output relations for the complete state transfer are known. They can be written in terms of creation and annihilation operators such that all occurring modes are independent. The transformation is of the type

$$U_N a_{in}^\dagger U_N^\dagger = \sum_{i=1}^n k_i a_i^\dagger + \sum_{j=1}^m k_j c_j, \quad (B2)$$

where the coefficients k_i , k_j are complex numbers. $a_1^\dagger = a_{in}^\dagger$ refers to the state to be stored, while a_2^\dagger to a_n^\dagger represent all creation operators which appear in the equation, namely contributions from the atomic input, atomic noise, light-input from the read-out beam and light noise. Since we also have noise terms, which cannot be expressed as a noise mode (compare equation (A4) last term) and contributions from the lower sideband (compare equation (A5)) in which the x - and p quadratures are interchanged, we also have annihilation operators in this equation which are represented by c_1 to c_j . Since these contributions are small, they are treated as perturbations to the system.

The transformation given in (B2) can be understood as an orthogonal transformation $P = P_a \otimes P_c$, where P_a acts on the creation operators and P_c acts on the annihilation operators, followed by an active transformation S . With normalization constants $N_a = \sqrt{\sum_{i=1}^n |k_i|^2}$ and

$N_c = \sqrt{\sum_{j=1}^m |k_j|^2}$, where $N_a^2 - N_c^2 = 1$ and $N_c \ll 1$, (B2) can be written as

$$a_{fin}^\dagger = N_a \left(\sum_{i=1}^n \frac{k_i}{N_a} a_i^\dagger \right) + N_c \left(\sum_{j=1}^m \frac{k_j}{N_c} c_j \right) \quad (\text{B3})$$

$$= N_a P_a a_1^\dagger P_a^\dagger + N_c P_c c_1 P_c^\dagger = N_a a_P^\dagger + N_c c_P \quad (\text{B4})$$

and we have $U_N = S(P_a \otimes P_c)$. In order to compute F_{qubit} from equation (B1) the expression $U_N|vac\rangle$ has to be determined. $U_N|vac\rangle = S(P_a \otimes P_c)|vac\rangle = S|vac\rangle$, since P is a passive transformation. S on the other hand refers to a two mode squeezing operation. As mentioned above active contributions are treated perturbatively. The corresponding time evolution $S = e^{N_c(a_P c - a_P^\dagger c^\dagger)}$ is expanded

in a series to first order and we obtain

$$U_N|vac\rangle = \frac{1}{\sqrt{1+|N_c|^2}} (1 - N_c a_P^\dagger c_P^\dagger)|vac\rangle$$

By inserting this expression in equation (B1) and inserting the right hand side of (B2) for a_{fin}^\dagger the fidelity can be directly calculated. We find

$$F_{qubit} = \frac{1}{1+|N_c|^2} \left(|\alpha|^2 - |\beta|^2 k_1 \left(1 - \frac{|N_c|^2}{\sqrt{1+|N_c|^2}} \right) \right)^2.$$

In order to obtain the average fidelity we set $\alpha = \cos(\frac{\theta}{2})$ and $\beta = \sin(\frac{\theta}{2})e^{i\phi}$ and integrate over the whole Bloch sphere $\bar{F}_{qubit} = \frac{1}{4\pi} \int_0^\pi \int_0^{2\pi} F_{qubit}(\theta, \phi) \sin(\theta) d\theta d\phi$. The results are shown in figures 7 and 8.

-
- [1] C.W. Chou, H. de Riedmatten, D. Felinto, S.V. Polyakov, S.J. van Enk, H.J. Kimble, *Nature* **438**, 828 (2005)
[2] T. Chanelire, D.N. Matsukevich, S.D. Jenkins, S.-Y. Lan, T.A.B. Kennedy, A. Kuzmich, *Nature* **438**, 833 (2005)
[3] M.D. Eisaman, A. Andr, F. Massou, M. Fleischhauer, A.S. Zibrov, M. D. Lukin, *Nature* **438**, 837 (2005)
[4] B. Julsgaard, J. Sherson, J.I. Cirac, J. Fiurasek, E.S. Polzik, *Nature* **432**, 482 (2004)
[5] S.L. Braunstein, A. K. Pati (eds.), *Quantum Infomation with Continuous Variables* (Kluwer, Dordrecht, 2003)
[6] A. Kuzmich and E. S. Polzik, *Quantum Infomation with Continuous Variables* (Kluwer, Dordrecht, 2003), pp. 231265, eds. S. L. Braunstein and A. K. Pati.
[7] B. Kraus, K. Hammerer, G. Giedke, J. I. Cirac, *Phys. Rev. A* **67**, 042314 (2003)
[8] K. Hammerer, K. Molmer, E.S. Polzik, J.I. Cirac, *Phys. Rev. A* **70**, 044304 (2004)
[9] J. Fiurasek, *Phys. Rev. A* **68**, 022304 (2003)
[10] J. Sherson, A.S. Sorensen, J. Fiurasek, K. Molmer, E.S. Polzik, *quant-ph/0505170*
[11] J. Fiurasek, J. Sherson, T. Opatrny, E.S. Polzik, *quant-ph/0510099*
[12] B. Julsgaard, A. Kozhekin, E.S. Polzik, *Nature* **413**, 400 (2001)
[13] A.S. Parkins, E. Solano, J.I. Cirac *quant-ph/0510173*
[14] A. Dantan, J.Cviklinski, M. Pinard, P. Grangier *quant-ph/0512175*
[15] L.-M. Duan, J.I. Cirac, M. Lukin, P. Zoller, *Nature* **414**, 413 (2001)
[16] T. Holstein, H. Primakoff, *Phys. Rev.* **58**, 1098 (1940)
[17] L.-M. Duan, J.I. Cirac, P. Zoller, E.S. Polzik, *Phys. Rev. Lett.* **85**, 5643 (2000)
[18] K. Hammerer, E. S. Polzik, J.I. Cirac, *Phys. Rev. A* **72**, 052313 (2005)
[19] B. Julsgaard, *Entanglement and Quantum Interactions with Macroscopic Gas Samples*, PhD Thesis, October 2003, Aarhus University, Denmark, <http://www.nbi.dk/~julsgard/>
[20] S.L. Braunstein, H.J. Kimble, C.A. Fuchs, *J. Mod. Opt.* **47**, 267 (2000)
[21] K. Hammerer, M.M. Wolf, E.S. Polzik, J.I. Cirac, *Phys. Rev. Lett.* **94**, 150503 (2005)
[22] S. Popescu, *Phys. Rev. Lett.* **72**, 797 (1994)
[23] S. Massar and S. Popescu, *Phys. Rev. Lett.* **74**, 1259 (1995)
[24] R. Derka *et al.* *Phys. Rev. Lett.* **80**, 1571 (1998)
[25] D. Bruss *et al.* *Phys. Rev. Lett.* **81**, 2598 (1998)
[26] G. Giedke, M.M. Wolf, O. Kriger, R. F. Werner, J.I. Cirac *Phys. Rev. Lett.* **91**, 107901 (2003)